Arabian Journal of Chemistry (2020) **13**, 7055–7065

King Saud University

Arabian Journal of Chemistry

www.ksu.edu.sa
www.sciencedirect.com

ORIGINAL ARTICLE

Comprehensive analysis of resveratrol metabolites in rats using ultra high performance liquid chromatography coupled with high resolution mass spectrometry

Zihan Liu [a,b], Shaoping Wang [b], Fan Dong [a,b], Ying Lin [b], Haoran Li [c], Lei Shi [c], Zhibin Wang [d,*], Jiayu Zhang [b,*]

[a] *School of Chinese Pharmacy, Beijing University of Chinese Medicine, Beijing 102488, China*
[b] *School of Pharmacy, BIN ZHOU Medical University, 264003, China*
[c] *Shandong University of Traditional Chinese Medicine, Jinan 250300, China*
[d] *Tongrentang Research Institute, Beijing 100079, China*

Received 18 May 2020; accepted 12 July 2020
Available online 21 July 2020

KEYWORDS

Resveratrol;
Metablite;
UHPLC-LTQ-Orbitrap MS;
Metabolic network

Abstract Resveratrol is an antitoxin secreted by plants such as *Polygonum cuspidatum Sieb. et Zucc* and *Vitis vinifera L.* when they are attacked by pathogens. In the present study, three methods were used to prepare biological samples, and then an efficient strategy based on ultra-high-performance liquid chromatography-linear ion trap-Orbitrap mass spectrometry (UHPLC-LTQ-Orbitrap MS) was developed to screen and identify resveratrol metabolites in rat urine, plasma and faeces. As a result, a total of 56 resveratrol metabolites were screened and characterized. Among them, 39 metabolites were found in rat urine, while 6 and 16 metabolites were characterized from rat plasma and faeces, respectively. In addition, 56, 12 and 15 metabolic products were screened by solid phase extraction (method I), methanol precipitation (method II) and acetonitrile precipitation (method III), respectively, indicating that method I could be adopted as the most acceptable method. The results also demonstrated that resveratrol mainly underwent glucuronidation, glucosylation, sulfation, hydroxylation, dehydrogenation, hydrogenation, methylation and their composite reactions. Moreover, these metabolic reactions occurred to form a possible meta-

* Corresponding authors.
E-mail addresses: wangzhibin@tongrentang.com (Z. Wang), zhangjiayu0615@163.com (J. Zhang).
Peer review under responsibility of King Saud University.

Production and hosting by Elsevier

https://doi.org/10.1016/j.arabjc.2020.07.011

bolic network that is similar to a triangular pyramid model. In summary, this research provides an idea for the further study of drug metabolism.

1. Introduction

Resveratrol is a natural polyphenolic, non-flavonoid antioxidant produced by many herbal plants, such as *Polygonum cuspidatum* Sieb. et Zucc and *Vitis vinifera* L., during the process of reacting to a stimulus (Samarjit and Dipak, 2007). Resveratrol has been reported to have widespread biological activities, including antitumour (Patel et al., 2010), antioxidant (Xu et al., 2020), anti-inflammatory (Chen et al., 2020) and cardiovascular protection (Fremont, 2000). Similarly, resveratrol plays an important role in anti-inflammatory reactions by inhibiting the secretion of nitric oxides and TNF-α in N9 microglial cells and cortical microglia (Bergman et al., 2013). Resveratrol has also shown a positive effect on immune function, since it may be involved in the specific and non-specific immune response by directly regulating lymphocyte, macrophage and dendritic cell activation (Svajger and Jeras, 2012). Thus, resveratrol has been extensively adopted as a significant additive in food, cosmetics, medicine, health care and other fields.

Metabolism studies *in vivo* have been an important means to clarify the mechanism of action of the drug and provide an important basis to guide clinical medication recommendations (Sandermann, 1992; Wilkinson, 2005). M. Emília Juan et al. developed a methodology for the extraction and quantification of *trans*-resveratrol and its metabolites in the plasma, brain, testis, liver, lungs and kidney based on HPLC analysis (Emília Juan et al., 2010). A reversed-phase HPLC method proposed by David J et al. was applied to determine the levels of resveratrol and identify six major conjugated metabolites in the plasma and urine of human volunteers (Boocock et al., 2007). Nevertheless, there were shortages in resveratrol metabolite quantity and their related descriptions by the above methods. However, a problem that cannot be ignored in metabolism studies is that metabolites are often found in small quantities and hence are usually hard to detect (Shang et al., 2017). Therefore, it is necessary to obtain a complete chemical characterization of resveratrol metabolites and to develop sensitive, accurate and high-resolution methods for their qualitative analyses.

Over the last decade, establishing an efficient and powerful analytical method for identifying drug metabolites has been of great significance with the rapid development of ultra-high-performance liquid chromatography coupled with high-resolution mass spectrometry (UHPLC-HRMS). Moreover, the coverage of metabolite screening and the abundance of ESI-MS/MS information can increase by using the full scan-parent ion list-dynamic exclusion (FS-PIL-DE) method coupled to diagnostic product ion (DPI) analysis on a hybrid LTQ-Orbitrap mass spectrometer (Zhang et al., 2014; Xu et al., 2017; Dai et al., 2017). Two-step mass defect filtering-induced exclusion list-data dependent acquisition was established on the basis of two-dimensional liquid chromatography coupled with quadrupole-Orbitrap mass spectrometer, which further increased MS/MS coverage and selectivity (Pan et al., 2020). A multiplicate strategy, PIL in full MS/dd-MS^2 to detect targeted components and "if idle-pick others" for distinguishing the MS^2 information of those untargeted ones, developed on a high-resolution Q Exactive hybrid quadrupole-Orbitrap mass spectrometer coupled to offline comprehensive 2D-LC. It benefits the simultaneous identification and characterization of the targeted and untargeted metabolites (Fu et al., 2019). Herein, we established an UHPLC-LTQ-Orbitrap MS-based strategy to perform the comprehensive identification and characterization of resveratrol metabolites in the plasma, urine and faeces of Sprague-Dawley (SD) rats following intragastric administration of resveratrol.

2. Experiment

2.1. Chemicals and materials

Resveratrol and polydatin were purchased from Chengdu Must Biotechnology Co. Ltd (Sichuan, China). These reference standards with purities higher than 98% were applicable to UHPLC-LTQ-Orbitrap analysis.

HPLC grade acetonitrile, methanol and formic acid were purchased from Thermo Fisher Scientifific (Fair Lawn, NJ, USA). All the other chemicals of analytical grade were available at the work station, Beijing Chemical Works (Beijing, China). Deionized water used throughoutthe experiment was purifified by a Milli-Q Gradient Å 10 System (Millipore, Billerica, MA, USA). Grace Pure™SPE C_{18}-Low solid phase extraction cartridges (200 mg/3 mL, 59 μm, 70 Å) were purchased from Grace Davison Discovery Science (Deerfifield, IL, USA).

2.2. Animals

Eight male SD rats weighted 200 ± 20 g were obtained from Beijing Weitong Lihua Experimental Animals Company (Beijing, China). The rats were housed in a controlled room at standard temperature (24 ± 2 °C) and humidity (70 ± 5%), and kept on a 12 h light/12 h dark regime. After a week acclimation, rats were randomly divided into two groups: Drug Group (n = 4) for test plasma, urine and feces; Control Group (n = 4) for blank plasma, urine and feces. They were fasted for 12 h with free access to water prior to the experiment. The animal protocols were approved by the institutional Animal Care and Use Committee at Beijing University of Chinese Medicine. The animal facilities and protocols were complied with the Guide for the Care and Use of Laboratory Animals.

2.3. Drug administration and biological sample preparation

Resveratrol was suspended in 0.5% carboxymethylcellulose sodium (CMC-Na) solution and given at a dose of 300 mg/kg body weight to rats in the drug group. A 0.5% CMC-Na aqueous solution (2 mL) was parallelly administered to rats

in the control group. Blood samples (0.5 mL) were taken from the suborbital venous plexus of rats at 0.5, 1, 2 and 4 h post-administration. Each sample was centrifuged at 3 500 rpm for 10 min to obtain plasma samples. Urine and faecal samples were collected 0–24 h after intragastric administration. All homogeneous biological samples from the same group were finally merged into a collective sample.

Different processing methods were used to pretreat the collected blood, urine and faecal samples. The first method (method I) was performed to prepare biological samples by solid phase extraction (SPE). Plasma and urine samples (1 mL) were added to an SPE cartridge pretreated with methanol (5 mL) and deionized water (5 mL). Then, the SPE cartridges were successively washed with deionized water (5 mL) and methanol (3 mL). The methanol eluate was collected and evaporated by nitrogen at room temperature. The residue was redissolved in 100 μL of acetonitrile/water (10:90, v/v) and then centrifuged at 14,000 rpm for 15 min. Faecal samples (1.0 g) were ultrasonically extracted with deionized water (5.0 mL) for 15 min and then filtered. The supernatant (1 mL) was added to the pretreated SPE cartridge, and then the same process described above was conducted. The second method (method II) used methanol to precipitate the supernatants of the faeces, blood and urine samples. The proportion of methanol to these samples was 1:3. These samples were precipitated for 30 min and then centrifuged at 14,000 rpm for 15 min to obtain the solutions after treatment. The third method (method III) used acetonitrile to precipitate the above biological samples. The ratio of acetonitrile to sample was also one to three, and then the same process described in method II was carried out. All the supernatants were used for further instrumental analysis.

2.4. Instrument and conditions

LC analysis was performed on a DIONEX Ultimate 3000 UHPLC system (Thermo Electron, Bremen, Germany), equipped with a binary pump and an auto-sampler. The chromatographic separation was carried out using Waters ACQUITY BEH C18 column (2.1 × 100 mm i.d., 1.7 μm; Waters Corporation, Milford, MA, USA) at 35 °C. Methanol (solvent B) and 0.1% formic acid aqueous solution (solvent A) were used as mobile phase. The flow rate was set to 0.3 mL/min with a linear gradient as follows: 0–2 min, 25% B; 2–11 min, 25–55% B; 11–17 min, 55–95% B. The injection volume was 2 μL.

High resolution ESI-MS and MS/MS spectra were obtained using LTQ-Orbitrap MS (Thermo Electron, Bremen, Germany) connected to the UHPLC instrument *via* ESI interface. Samples were analyzed in negative ion mode with the tune method set as follows: sheath gas (nitrogen) flow rate of 40 arb, auxiliary gas (nitrogen) flow rate of 20 arb, capillary temperature of 350 °C, spray voltage of 4.0 kV, capillary voltage of 25 V, tube lens voltage of 110 V. Metabolites were detected using full-scan MS analysis from *m/z* 50-800 at a resolving power of 30,000 FWHM. The collision energy for collision induced dissociation (CID) was adjusted to 40% of maximum. In addition, the PIL-dependent acquisition mode was employed as a complementary tool to obtain the ESI-MS/MS dataset of potential metabolites.

2.5. Peak selections and data processing

Thermo Xcalibur 2.1 workstation was used for data acquisition and processing. In order to obtain as many ESI-MS/MS fragment ions of resveratrol metabolites as possible, the peaks detected with intensity over 10,000 were selected for identification. The accurate mass of chemical formulas attributed to all parent ions of the selected peaks were calculated using a formula predictor by setting the parameters as follows: C [0–35], H [0–40], O [0–16], S [0–1] and ring double bond (RDB) equivalent value [0–14]. Accurate mass measurements were set within mass error of ± 5 ppm.

3. Results and discussion

3.1. The establishment of analytical strategy

In this study, all the collected biological samples (urine, plasma and faeces) were prepared using the three abovementioned methods, which included solid phase extraction, methanol precipitation and acetonitrile precipitation. Then the samples were injected into UHPLC-Q-Exactive Orbitrap MS to gain the HRMS data with full MS scanning acquisition. Then, data mining was processing based on common biotransformation reactions as well as the reported metabolites in literature. And subsequently, the ions which we were interested in were put into PIL to obtain more comprehensive MS2 information for structural identification. Among them, polydatin, dihydroresveratrol and pterostilbene were also regarded as pivotal candidate metabolites and filled into PIL. Finally, an efficient analysis based on UHPLC-LTQ-Orbitrap MS coupled with FS-PIL-DE was proposed to characterize and screen the metabolic products. Combining the chromatographic retention behaviours, accurate mass measurements, mass fragmentation patterns and previous relevant literature, was conducive to the comprehensive analysis of the metabolites of the resveratrol representative chemical components. In addition, a diagram that summarizes the presently developed analytical strategy and methodology for the detection and identification of resveratrol metabolites is shown in Fig. 1.

3.2. Fragmentation patterns analysis of resveratrol

In order to better characterize the *in vivo* metabolites, DPIs were essential for structural identification. Resveratrol was selected as the subject to determine its DPIs based on the comprehensive ESI-MS^n information of the resveratrol standard via UHPLC-HRMS analysis. For example, resveratrol gave rise to deprotonated $[M-H]^-$ ions at *m/z* 227.07057, as shown in Fig. 2. Then, it would further afford a series of DPIs at *m/z* 185, 159 and 143 owing to the loss of C_2H_2O (42 Da), $C_2H_2O + C_2H_2$ (68 Da) and $2C_2H_2O$ (84 Da) (Wang et al., 2005; Mei et al., 2019). Therefore, the product ions of resveratrol metabolites at *m/z* 185 + X, *m/z* 159 + X and *m/z* 143 + X (X = molecular weight of the substituent groups), such as 14 (CH_2), 80 (SO_3), and 176 (GluA), could also be observed in the ESI-MS/MS spectra.

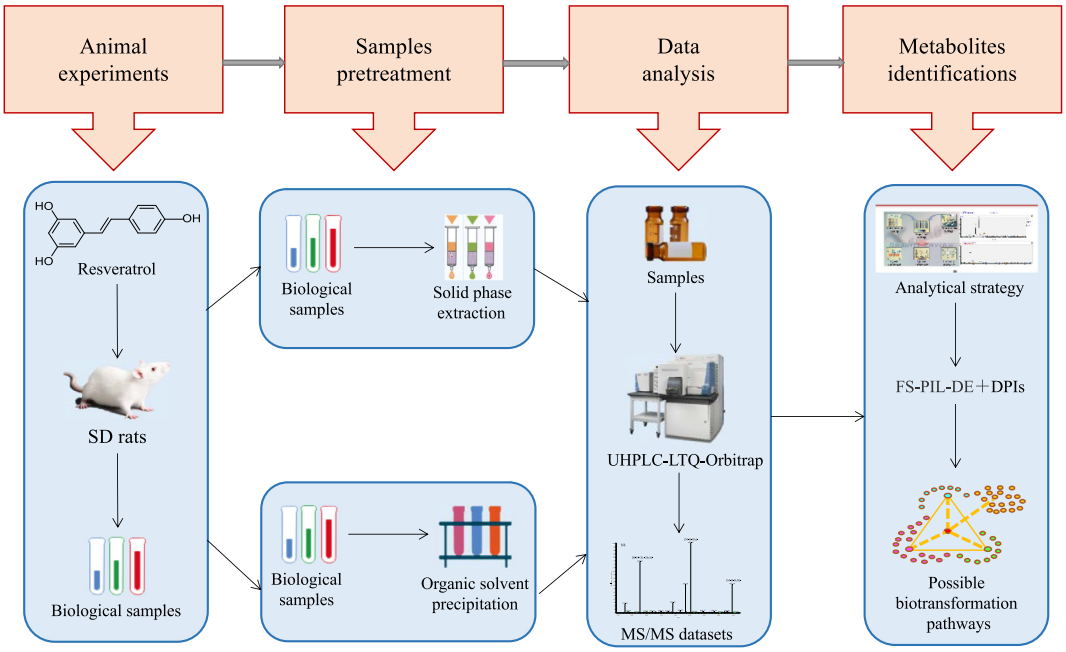

Fig. 1 The summary diagram of analytical strategy and methodology.

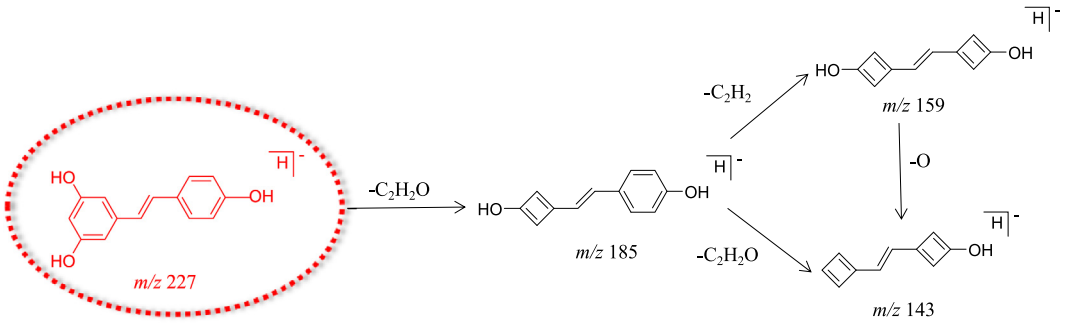

Fig. 2 The proposed fragmentation pathways of resveratrol.

3.3. Identification of resveratrol metabolites

A total of 56 resveratrol metabolites (resveratrol included) were detected and characterized from rat urine, plasma and faecal samples by means of the UHPLC-LTQ-Orbitrap method coupled with the established strategy. Among them, 39 metabolites were found in rat urine, 6 metabolites were detected in rat plasma, and 16 metabolites were characterized from rat faeces. The correlative data in negative ion mode are summarized in Table 1.

Metabolites **N1**, **N2**, **N25**, **N29** and **N34** possessed deprotonated molecular ions at *m/z* 243.06580, *m/z* 243.06572, *m/z* 243.06593, *m/z* 243.06587, and *m/z* 243.06572 ($C_{14}H_{11}O_4$) with mass errors of 2.529, 2.200, 3.064, 2.817 and 3.269 ppm, respectively. Fragment ions at *m/z* 201 $[M-H-C_2H_2O]^-$, *m/z* 175 $[M-H-C_2H_2O-C_2H_2]^-$ and *m/z* 159 $[M-H-2C_2H_2O]^-$ were all observed in the ESI-MS^2 spectra. In addition, their $[M-H]^-$ ions at *m/z* 243 were 16 Da more than that of resveratrol, which implied the occurrence of a hydroxylation reaction. Thus, **N1**, **N2**, **N25**, **N29** and **N34** were plausibly assigned as hydroxylated resveratrol.

N3 and **N4** afforded $[M-H]^-$ ions at *m/z* 137.02394 and *m/z* 137.02321 ($C_7H_5O_3$, mass errors 4.521 ppm and −0.807 ppm), respectively. They generated ESI-MS^2 DPIs at *m/z* 93 and *m/z* 109 due to the neutral loss of CO_2 and CO, which indicated the presence of carboxyl groups. Therefore, **N3** and **N4** could be deduced as isomeric 4-hydroxybenzoic acid.

N5 was 194 Da greater than that of dihydroresveratrol, which displayed an $[M-H]^-$ ion at *m/z* 421.11301 with a mass error of 0.206 ppm. In its ESI-MS^2 spectrum, the deprotonated molecular $[M-H]^-$ ion at *m/z* 421 further generated several product ions at *m/z* 245 $[M-H-GluA]^-$ and *m/z* 175 $[GluA-H]^-$. Based on this, **N5** was identified as glucuronidation and hydroxylation product of dihydroresveratrol.

Six isomeric constituents, **N6**, **N12**, **N13**, **N17**, **N22** and **N48**, gave rise to $[M-H]^-$ ions at *m/z* 323.02252, *m/z* 323.02237, *m/z* 323.02264, *m/z* 323.02255, *m/z* 323.02261 and

Table 1 Summary of resveratrol metabolites in rat urine, plasma and feces.

Peak	t_R (min)	Formula $[M + H]^+$	Theoretical Mass (*m/z*)	Experimental Mass (*m/z*)	RDB	Error (ppm)	MS/MS fragment ions	Identification/ Reactions	U	P	F
N1	1.91	$C_{14}H_{11}O_4$	243.06572	243.06580	9.5	2.529	173(100),201(56),212 (47),199(18),145(14),198 (14),225(11)	resveratrol hydroxylation/isomer	+		
N2	2.74	$C_{14}H_{11}O_4$	243.06636	243.06572	9.5	2.200	201(100),215(41),199 (30),109(28),225(25),181 (15),173(10)	resveratrol hydroxylation/isomer	+		
N3	3.03	$C_7H_5O_3$	137.02456	137.02394	5.5	4.521	93(100),137(55),109 (8),95(5),117(3)	4-hydroxybenzoic acid	+		
N4	3.59	$C_7H_5O_3$	137.02456	137.02321	5.5	−0.807	137(100),93(91),119 (19),95(18),109(14),106 (14)	4-hydroxybenzoic acid	+		+
N5	3.61	$C_{20}H_{21}O_{10}$	421.11399	421.11301	10.5	0.206	403(100),175(99),341 (23),245(21),333(17),302 (15)	dihydroresveratrol glucuronidation, hydroxylation	+		
N6	3.65	$C_{14}H_{11}O_7S$	323.02306	323.02252	9.5	1.610	243(100),244(5),241 (3),267(2),278(1)	resveratrol sulfation, hydroxylation/isomer			+
N7	3.71	$C_{26}H_{29}O_{14}$	565.15629	565.15515	12.5	−0.056	403(100),227(74),547 (65),175(56),341(38),389 (37)	resveratrol glucosylation, glucuronidation	+		
N8	3.91	$C_{26}H_{29}O_{14}$	565.15629	565.15533	12.5	0.262	403(100),227(73),547 (71),385(41),341(14),175 (12)	resveratrol glucosylation, glucuronidation	+		
N9	3.95	$C_{26}H_{27}O_{15}$	579.13556	579.13428	13.5	−0.287	403(100),175(1)	resveratrol bis-glucuronidation	+		
N10	3.96	$C_{26}H_{29}O_{15}$	581.15119	581.15100	12.5	1.555	403(100),534(2),175 (2),535(1)	dihydroresveratrol bis-glucuronidation	+		
N11	4.05	$C_{20}H_{21}O_{11}S$	469.08099	469.08044	10.5	1.133	227(100),389(29),307 (9),306(8),405(8),243(5)	resveratrol glucosylation, sulfation	+		
N12	4.11	$C_{14}H_{11}O_7S$	323.02306	323.02237	9.5	1.146	243(100),306(10),189 (6),203(6)	resveratrol sulfation, hydroxylation/isomer	+		
N13	4.22	$C_{14}H_{11}O_7S$	323.02306	323.02264	9.5	1.982	243(100),244(8)0.295 (7),241(6),189(4)	resveratrol sulfation, hydroxylation/isomer			+
N14	4.28	$C_{20}H_{21}O_{11}S$	469.08099	469.07977	10.5	−0.295	227(100),307(18),241 (10),269(6)	resveratrol glucosylation, sulfation	+		
N15	4.45	$C_{20}H_{19}O_9$	403.10339	403.10275	11.5	0.971	384(100),385(71),374 (12),227(12),375(11),175 (9)	resveratrol glucuronidation/ isomer	+		
N16	4.67	$C_{20}H_{19}O_{10}$	419.09836	419.09790	11.5	1.496	243(100),175(22),401(3)	resveratrol hydroxylation, glucuronidation	+		
N17	4.70	$C_{14}H_{11}O_7S$	323.02306	323.02255	9.5	1.703	243(100),295(16),241 (12),244(9),225(4)	resveratrol sulfation, hydroxylation/isomer			+
N18	4.78	$C_{20}H_{21}O_{11}S$	469.08099	469.08044	10.5	1.133	227(100),307(16),269 (3),185(2)	resveratrol glucosylation, sulfation	+		
N19	4.78	$C_{26}H_{29}O_{14}$	565.15629	565.15515	12.5	−0.056	337(100),385(26),179 (17),227(16),175(8),237 (7)	resveratrol glucosylation, glucuronidation	+		
N20*	4.80	$C_{20}H_{21}O_8$	389.12416	389.12402	10.5	2.380	175(100),385(28),227 (21),323(10)	polydatin		+	
N21	4.87	$C_{20}H_{19}O_9$	403.10346	403.10269	11.5	0.822	175(100),227(36),385 (20),341(4)	resveratrol glucuronidation/ isomer	+	+	
N22	5.01	$C_{14}H_{11}O_7S$	323.02306	323.02261	9.5	1.889	243(100),259(2),241(1)	resveratrol sulfation, hydroxylation/isomer			+
N23	5.10	$C_{14}H_{11}O_6S$	307.02816	307.02789	9.5	2.621	227(100),228(1)	resveratrol sulfation/ isomer			+
N24	5.24	$C_{14}H_{11}O_6S$	307.02816	307.02713	9.5	0.146	227(100),243(8)	resveratrol sulfation/ isomer	+		

(*continued on next page*)

Table 1 (*continued*)

Peak	t_R (min)	Formula $[M + H]^+$	Theoretical Mass (*m/z*)	Experimental Mass (*m/z*)	RDB	Error (ppm)	MS/MS fragment ions	Identification/ Reactions	U	P	F
N25	5.29	$C_{14}H_{11}O_4$	243.06572	243.06593	9.5	3.064	225(100),201(63),199 (38),175(31),200(18),159 (16)	resveratrol hydroxylation/isomer			+
N26	5.46	$C_{14}H_{11}O_6S$	307.02816	307.02695	9.5	−0.440	227(100),243(10)	resveratrol sulfation/ isomer	+		
N27	5.54	$C_{20}H_{21}O_8$	389.12416	389.12427	10.5	3.022	175(100),385(34),227 (14),359(11)	polydatin/isomer		+	
N28	5.55	$C_{20}H_{19}O_9$	403.10346	403.10364	11.5	3.179	175(100),385(34),227 (14),359(11)	resveratrol glucuronidation/ isomer		+	
N29	5.56	$C_{14}H_{11}O_4$	243.06572	243.06587	9.5	2.817	225(100),201(65),199 (34),175(33),200(17),215 (16)	resveratrol hydroxylation/isomer			+
N30	5.59	$C_{14}H_{11}O_6S$	307.02816	307.02771	9.5	2.035	227(100),243(8),289(1)	resveratrol sulfation/ isomer			+
N31	5.64	$C_{14}H_{11}O_6S$	307.02816	307.02800	9.5	2.979	227(100),243(13),228(2)	resveratrol sulfation/ isomer		+	
N32	5.81	$C_{15}H_{13}O_4$	257.08186	257.08115	9.5	1.224	241(100),242(49),224 (17),172(11),147(9)	resveratrol methylation, hydroxylation/isomer	+		
N33	5.81	$C_{20}H_{19}O_9$	403.10346	403.10233	11.5	−0.071	175(100),227(23),385 (17),244(4),384(3)	resveratrol glucuronidation/ isomer	+		
N34	5.85	$C_{14}H_{11}O_4$	243.06572	243.06598	9.5	3.269	225(100),201(63),199 (38),175(32),200(18),215 (16)	resveratrol hydroxylation/isomer			+
N35	6.03	$C_{20}H_{19}O_9$	403.10346	403.10248	11.5	0.301	175(100),227(28),385 (22),341(4),345(4)	resveratrol glucuronidation/ isomer	+		
N36	6.09	$C_{14}H_{11}O_3$	227.07136	227.07103	9.5	3.344	185(100),183(42),159 (32),157(27),143(16),227 (14),209(8)	resveratrol/isomer			+
N37	6.09	$C_{20}H_{21}O_8$	389.12416	389.12375	10.5	1.686	345(100),289(72),307 (46),371(21),306(11)	polydatin/isomer			+
N38	6.25	$C_{14}H_{11}O_3$	227.07146	227.07065	9.5	1.670	185(100),183(40),159 (31),157(25),143(15),227 (15),141(5)	resveratrol/isomer	+		
N39	6.30	$C_{14}H_{11}O_6S$	307.02816	307.02747	9.5	1.253	227(100),243(7),289 (2),225(1)	resveratrol sulfation/ isomer	+		+
N40	6.39	$C_{14}H_9O_4$	241.05056	241.05030	10.5	3.172	213(100),223(27),199 (17),184(11),173(10),197 (5)	resveratrol hydroxylation, dehydrogenation		+	
N41	6.57	$C_{15}H_{13}O_4$	257.08186	257.08112	9.5	1.107	135(100),121(58),239 (29),109(24),147(14),242 (11)	resveratrol methylation, hydroxylation/isomer	+		+
N42	6.65	$C_{15}H_{13}O_4$	257.08186	257.08136	9.5	2.041	135(100),121(56),109 (54),242(37),239(35),241 (33),147(22)	resveratrol methylation, hydroxylation/isomer	+		
N43	6.65	$C_{14}H_{11}O_6S$	307.02816	307.02747	9.5	1.253	227(100),243(11)	resveratrol sulfation/ isomer	+		
N44*	6.68	$C_{14}H_{11}O_3$	227.07136	227.07057	9.5	1.318	185(100),183(40),159 (33),157(24),143(13),227 (12)	resveratrol	+		
N45	6.68	$C_{20}H_{19}O_9$	403.10339	403.10272	11.5	0.897	385(100),384(27),367 (19),387(6)	resveratrol glucuronidation/ isomer	+		
N46	7.64	$C_{14}H_{11}O_3$	227.07136	227.07083	9.5	2.463	185(100),183(39),159 (29),157(24),143(15),227 (13)	resveratrol/isomer	+		+
N47	7.84	$C_{20}H_{19}O_9$	403.10346	403.10287	11.5	1.269	175(100),385(72),323 (57),322(32),324(26),285 (25),359(24)	resveratrol glucuronidation/ isomer	+		

Table 1 (*continued*)

Peak	t_R (min)	Formula $[M + H]^+$	Theoretical Mass (*m/z*)	Experimental Mass (*m/z*)	RDB	Error (ppm)	MS/MS fragment ions	Identification/ Reactions	U	P	F
N48	7.99	$C_{14}H_{11}O_7S$	323.02306	323.02136	9.5	−1.981	149(100),279(45),243 (43),261(20),305(19),251 (14)	resveratrol sulfation, hydroxylation/isomer	+		
N49	8.06	$C_{14}H_{11}O_3$	227.07136	227.07089	9.5	2.727	185(100),183(46),159 (31),157(23),143(17),227 (12),181(5)	resveratrol/isomer	+		
N50	8.70	$C_{14}H_{11}O_3$	227.07136	227.07088	9.5	2.683	185(100),183(46),159 (29),157(27),143(17),227 (14),141(6)	resveratrol/isomer	+		
N51	9.64	$C_{15}H_{13}O_4$	257.08186	257.08142	9.5	2.274	109(100),239(95),213 (29),242(25),147(15),148 (14),136(13)	resveratrol methylation, hydroxylation/isomer	+		
N52	9.85	$C_{15}H_{13}O_4$	257.08186	257.08072	9.5	−0.449	239(100),221(10),195 (7),147(7),213(6),237 (5),242(5)	resveratrol methylation, hydroxylation/isomer			+
N53	9.86	$C_{20}H_{19}O_9$	403.10346	403.10260	11.5	0.599	175(100),385(88),323 (82),293(71),335(65),359 (56)	resveratrol glucuronidation/ isomer	+		
N54	9.92	$C_{14}H_{11}O_3$	227.07136	227.07092	9.5	2.859	185(100),183(42),159 (32),157(27),143(14),207 (12),212(12)	resveratrol/isomer	+		
N55	10.74	$C_{14}H_{11}O_3$	227.07136	227.07086	9.5	2.595	185(100),183(58),159 (43),157(36),143(13),227 (12),199(9)	resveratrol/isomer	+		
N56	12.18	$C_{14}H_{11}O_3$	227.07136	227.07088	9.5	2.683	185(100),183(60),157 (42),143(33),159(32),207 (20)	resveratrol/isomer	+		

Note: t_R: retention time; RDB: unsaturation; U: urine; P: plasm; F:feces; +: detected; *:unambiguously identification by comparing with the reference substances.

m/z 323.02136 ($C_{14}H_{11}O_7S$) with mass errors of 1.610, 1.146, 1.982, 1.703, 1.889 and −1.981 ppm, respectively. In the ESI-MS^2 spectra, the characteristic product ion at *m/z* 243 was generated by the loss of 80 (SO_3) from the deprotonated molecular $[M-H]^-$ ion at *m/z* 323. Moreover, **N6**, **N12**, **N13**, **N17**, **N22** and **N48** were 96 Da more than that of resveratrol. Therefore, **N6**, **N12**, **N13**, **N17**, **N22** and **N48** were isomeric sulfated and hydroxylated metabolites of resveratrol.

N7, **N8** and **N19** showed $[M-H]^-$ ions at *m/z* 565.15515, *m/z* 565.15533 and *m/z* 565.15515 ($C_{26}H_{29}O_{14}$, mass error −0.056, 0.262 and −0.056 ppm), respectively.

These peaks were 338 Da more than that of resveratrol, indicating that they could be deduced as glucosylated and glucuronidated metabolites of resveratrol. In addition, the fragment ions at *m/z* 547 $[M-H-H_2O]^-$, DPIs at *m/z* 403 $[M-H-Glc]^-$ and *m/z* 227 $[M-H-Glc-GluA]^-$ were all observed in the ESI-MS^2 spectra. Based on this, **N7**, **N8** and **N19** were tentatively identified as isomeric resveratrol glucosylated and glucuronidated metabolites.

N9 produced the theoretical $[M-H]^-$ ion at *m/z* 579.13428 ($C_{26}H_{27}O_{15}$, mass error −0.287 ppm) with the mass being 352 Da more than that of resveratrol and was formed by the bis-glucuronidation of resveratrol *in vivo*. Owing to the successive loss of GluA, the $[M-H]^-$ ion generated an ion at *m/z* 403 in the ESI-MS^2 spectrum. Therefore, **N9** could be deduced as a resveratrol bis-glucuronidated metabolite. Additionally, **N10** generated an $[M-H]^-$ ion at *m/z* 581.15100 ($C_{26}H_{29}O_{15}$, mass error 1.555 ppm). The ESI-MS^2 characteristic product ion $[GluA-H]^-$ at *m/z* 175 showed the loss of 176 (GluA). Moreover, its $[M-H]^-$ ions were 2 Da more than that of **N9**, revealing that the bis-glucuronidation reaction most likely occurred. Thus, **N10** was speculated to be a dihydroresveratrol bis-glucuronidation metabolite.

In negative ion mode, **N11**, **N14** and **N18** produced $[M-H]^-$ ions at *m/z* 469.08044, *m/z* 469.07977 and *m/z* 469.08044 with mass errors of 1.133, −0.295 and 1.133 ppm ($C_{20}H_{21}O_{11}S$), respectively. In the ESI-MS^2 spectra, the fragment ion at *m/z* 389 $[M-H-SO_3]^-$ indicated that a sulfation reaction occurred. In addition, the neutral loss of 162 Da (*m/z* 389 → *m/z* 227) demonstrated the existence of a glucosyl group. Therefore, **N11**, **N14** and **N18** were tentatively characterized as isomeric glucosylated and sulfated metabolites of resveratrol.

Eight isomers, **N15**, **N21**, **N28**, **N33**, **N35**, **N45**, **N47** and **N53**, were 176 Da more than that of resveratrol, which respectively afforded $[M-H]^-$ ions at *m/z* 403.10275, *m/z* 403.10269, *m/z* 403.10364, *m/z* 403.10233, *m/z* 403.10248, *m/z* 403.10272, *m/z* 403.10287, and *m/z* 403.10260 ($C_{20}H_{19}O_9$, mass errors 0.971, 0.822, 3.179, −0.071, 0.301, 0.897, 1.269 and 0.599 ppm), respectively. In their ESI-MS^2 spectra, the characteristic product ions at *m/z* 227 $[M-H-GluA]^-$ and *m/z* 175 $[GluA-H]^-$ were detected. Therefore, **N15**, **N21**, **N28**, **N33**, **N35**, **N45**, **N47** and **N53** were tentatively identified as glucuronidated resveratrol or its isomers (Zhou et al., 2009; Zhang et al., 2008).

N16 possessed theoretical $[M-H]^-$ ions at *m/z* 419.09790 ($C_{20}H_{19}O_{10}$, mass error 1.496 ppm). In the ESI-MS^2 spectra, a battery of fragment ions at *m/z* 243 $[M-H-GluA]^-$, *m/z*

175 [GluA-H]$^-$ and m/z 401 [M−H−H_2O]$^-$ provided substantial evidence for this deduction. From the abovementioned analysis, **N16** was tentatively judged as isomeric hydroxylation and glucuronidation metabolite of resveratrol.

N20, **N27** and **N37** displayed significant [M−H]$^-$ ions at m/z 389.12402, m/z 389.12427 and m/z 389.12375 ($C_{20}H_{21}O_8$, mass errors 2.380, 3.022 and 1.686 ppm), respectively. They generated a DPI ion at m/z 227 in their ESI-MS^2 spectra. In addition, their [M−H]$^-$ ions were 162 Da more than that of resveratrol, which indicated the occurrence of a glucosylation reaction. Based upon comparison of their ESI-MS/MS spectra and retention time with the corresponding reference standard, **N20** was characterized as polydatin, while **N27** and **N37** were identified as polydatin isomers (Fu et al., 2018).

N23, **N24**, **N26**, **N30**, **N31**, **N39** and **N43** showed [M−H]$^-$ ions at m/z 307.02789, m/z 307.02713, m/z 307.02695, m/z 307.02771, m/z 307.02800, m/z 307.02747, and m/z 307.02747 with mass errors of 2.621, 0.146, −0.440, 2.035, 2.979, 1.253 and 1.253 ppm, respectively. They were 80 Da more than that of resveratrol, which illustrated the existence of a sulfation reaction. Based upon the obtained high-resolution mass spectrometry data, they yielded DPIs at m/z 227 due to the loss of SO_3. Thus, **N23**, **N24**, **N26**, **N30**, **N31**, **N39** and **N43** were tentatively interpreted as isomeric sulfated metabolites of resveratrol.

N32, **N41**, **N42**, **N51** and **N52** yielded significant [M−H]$^-$ ions at m/z 257.08115, m/z 257.08112, m/z 257.08136, m/z 257.08142 and m/z 257.08072 ($C_{15}H_{13}O_4$, mass error 1.224,

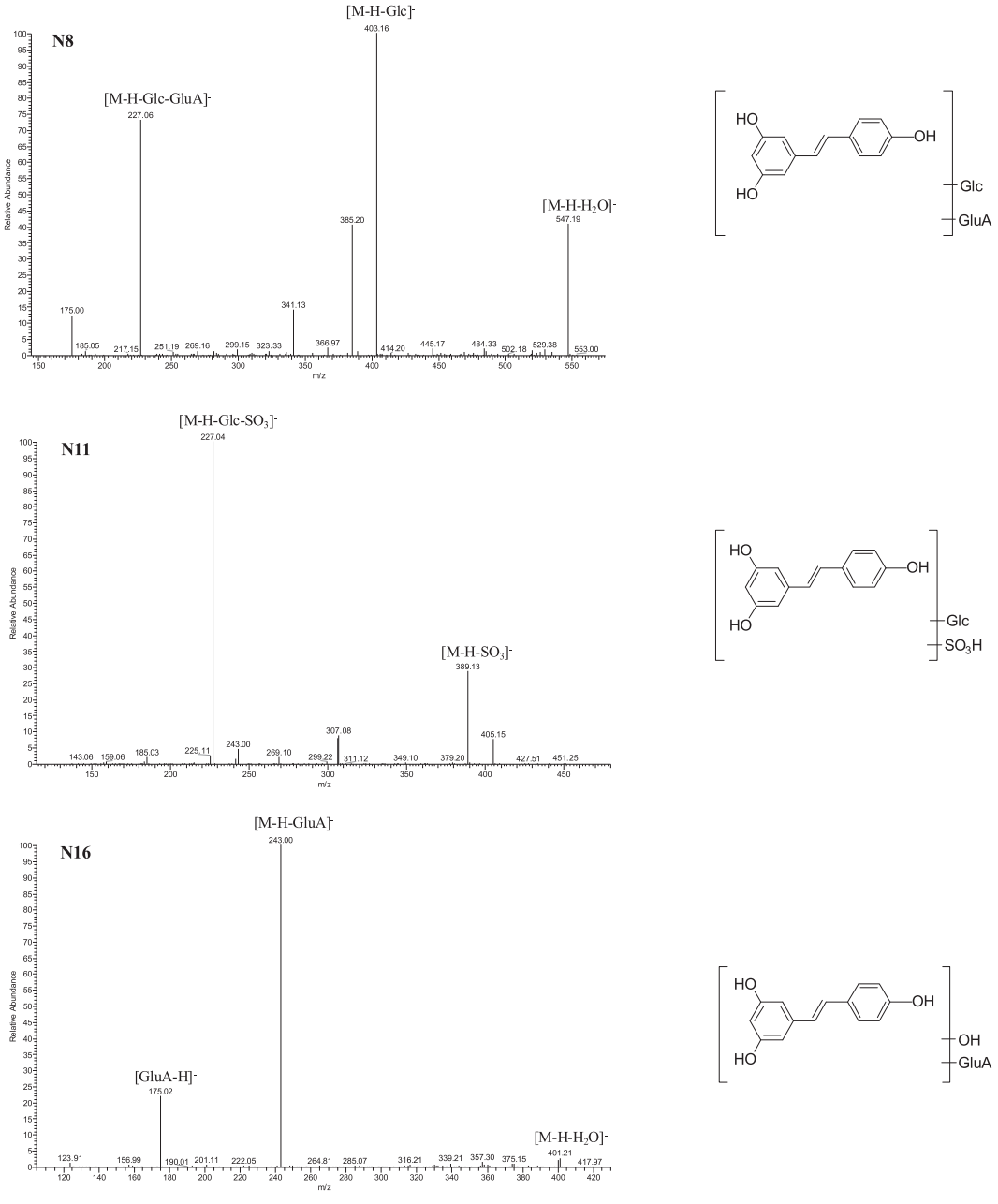

Fig. 3 The ESI-MS^2 spectra and chemical structures of **N8**, **N11** and **N16.**

1.107, 2.041, 2.274 and −0.449 ppm), respectively. They were 30 Da more than that of resveratrol, indicating that they could be methylated and hydroxylated metabolites of resveratrol. Moreover, they afforded DPIs at *m/z* 242 $[M-H-CH_3]^-$ and 147 $[M-H-2C_2H_2O-C_2H_2]^-$. According to the above deduction, **N32**, **N41**, **N42**, **N51** and **N52** were predicted to be methylated and hydroxylated metabolites of resveratrol.

Nine isomers, **N36**, **N38**, **N44**, **N46**, **N49**, **N50**, **N54**, **N55** and **N56**, gave rise to theoretical $[M-H]^-$ ions at *m/z* 227.07103, *m/z* 227.07065, *m/z* 227.07057, *m/z* 227.07083, *m/z* 227.07089, *m/z* 227.07088, *m/z* 227.07092, *m/z* 227.07086, *m/z* 227.07088 with mass errors of 3.344, 1.670, 1.318, 2.463, 2.727, 2.683, 2.859, 2.595 and 2.683 ppm, respectively. In the ESI-MS^2 spectra, there were many observed characteristic product ions at *m/z* 185, *m/z* 159 and *m/z* 143. Among them, the ion at *m/z* 185 $[M-H-C_2H_2O]^-$ was further fragmented to generate *m/z* 159 $[M-H-C_2H_2O-C_2H_2]^-$ and *m/z* 143 $[M-H-2C_2H_2O]^-$ after the loss of 26 Da and 42 Da, which were consistent with those documented in a previous report. Compared with the standard substance, **N44** was positively identified as resveratrol. From the above data, **N36**, **N38**, **N46**, **N49**, **N50**, **N54**, **N55** and **N56** were tentatively characterized as resveratrol isomers.

N40 generated a deprotonated molecular $[M-H]^-$ ion at *m/z* 241.05030 ($C_{14}H_9O_4$, mass error 3.172 ppm). It was 14 Da more than that of resveratrol, revealing that hydroxylation and dehydrogenation *in vivo* might have occurred. In its ESI-MS^2 spectra, DPIs at *m/z* 199 and *m/z* 173 were observed from the loss of C_2H_2O and C_2H_2O + C_2H_2. Therefore, **N40** was tentatively identified as an isomeric hydroxylated and dehydrogenated metabolite of resveratrol. In addition, the ESI-MS^2 spectra of **N8**, **N11** and **N16** are illustrated in Fig. 3**.**

3.4. Comparison of the different biological treatment methods

It should be noted that three methods were used to prepare the biological samples, and then the same analytical method was applied to detect the signals. According to the accurate mass measurements, fragmentation patterns, diagnostic product ions and literature reports, a total of 56 resveratrol phase I and phase II metabolites were screened and identified in rats by using the UHPLC-LTQ-Orbitrap method. Among them, 56 metabolic products were obtained by solid phase extraction, which was also named method I. Twelve and 15 metabolites were screened by methanol precipitation (method II) and acetonitrile precipitation (method III), respectively, as shown in Fig. 4.

As far as we know, the above three methods which bear a great significance in the pretreatment of biological materials are widely applied in various laboratories at present. On the basis of the results, it could be inferred that the majority of the metabolites were obtained by method I after the same detection analysis. It showed that the SPE cartridge was the most suitable method with the functions of enrichment and purification. In the preparation process, the target substance could be enriched, and then the impurities could be removed before instrumental analysis to improve analytical sensitivity and reduce damage to the instrument (Jordan et al., 2009; Nema et al., 2010). It might be deduced that SPE cartridge could provide much more effective and reliable support for removing matrix effect. After the sample was concentrated by SPE cartridge, more response signals could be detected in mass spectrometry. However, methanol and acetonitrile as organic solvents played the role of extraction and dilution in the process of sample precipitation, which might also indirectly lead to the concentration difference and undetection phenomenon. Furthermore, products of metabolism afforded by acetonitrile precipitation were slightly more abundant than those obtained by methanol precipitation, which indicated that acetonitrile might be more adaptive for resveratrol as a precipitation solvent than methanol. These differences in metabolites quantity might be due to the different separation selectivities of organic solvents, which lead to signal peaks with diverse intensity and quantity concerning resveratrol metabolites after UHPLC-HRMS detection.

3.5. Possible biotransformation pathways of resveratrol in rats

As"metabolite clusters" mentioned by Mei (Mei et al., 2019), resveratrol was regarded as the parent drug. When the parent drug was taken into the rat body, a series of metabolic

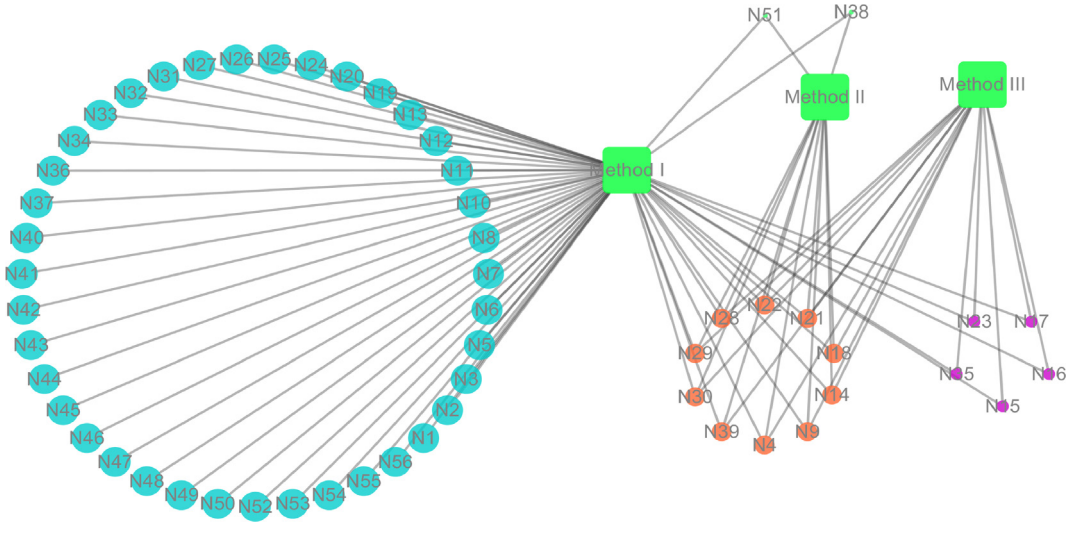

Fig. 4 The metabolic prodycts distribution of three biological treatment methods.

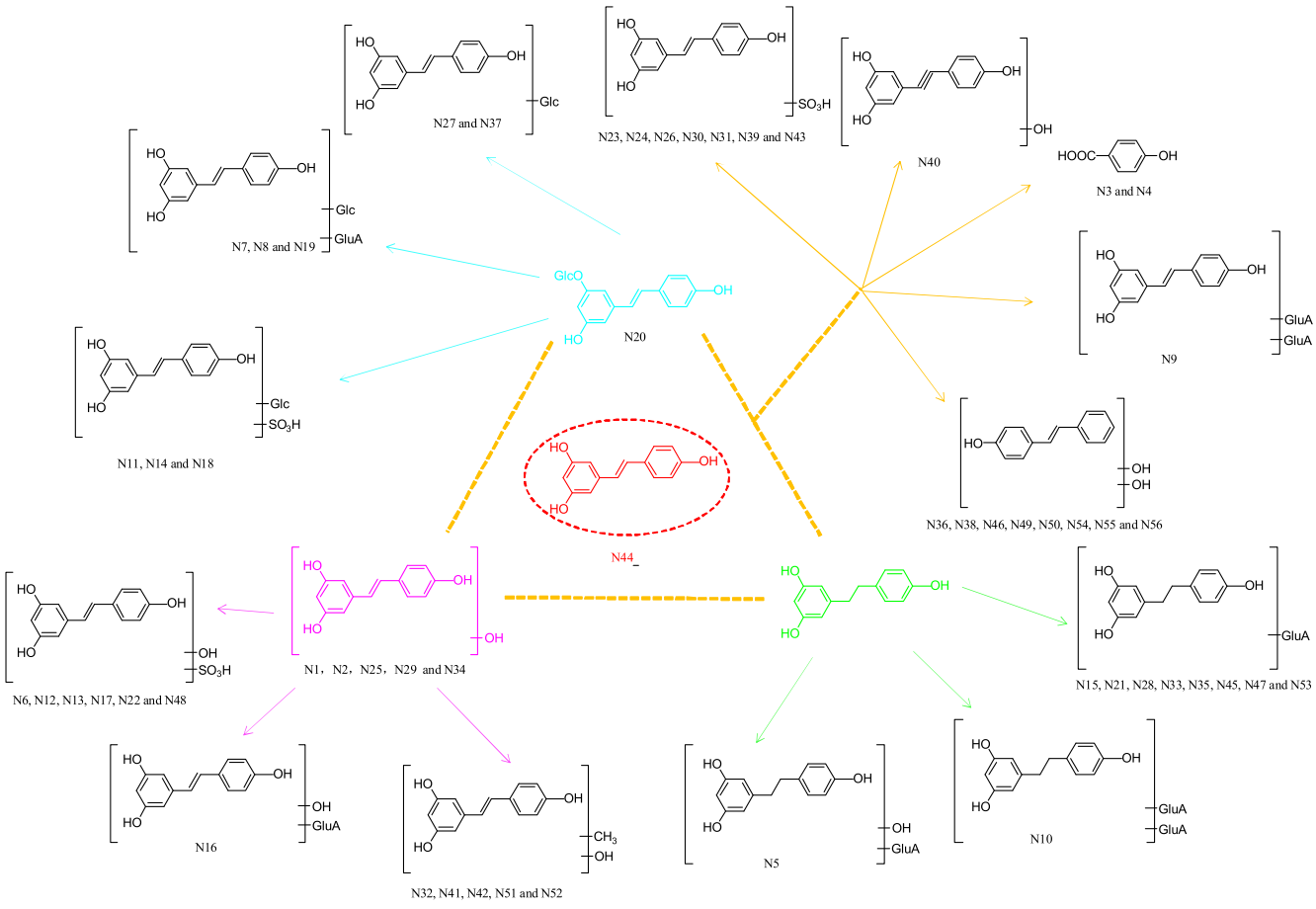

Fig. 5 The possible resveratrol metabolic patterns in rats *in vivo*.

reactions could occur to form a metabolic network similar to a triangular pyramid model (as shown in Figs. 5 and 6). These reactions could be roughly summarized as follows: the parent drug acted as the metabolic centre to generate secondary metabolic centres such as polydatin, dihydroresveratrol and hydroxylated resveratrol, and a great deal of final metabolites were derived from the secondary metabolic centres step by step. Among them, resveratrol mainly underwent glucuronidation, glucosylation, sulfation, hydroxylation, dehydrogenation, hydrogenation, methylation and their composite reactions. Phase II metabolism and its complicated reactions occupied the main status of these reactions. Of course, there were differences between the metabolic products and metabolic rates. More water-soluble metabolites, such as glucuronidated resveratrol and sulfated resveratrol, are generally produced through phase II reactions in order to prepare the drug for excretion (Wilkinson, 2005; Xu et al., 2005). It is also worth noting that the metabolic centres or the final metabolism products were not isolated. There might be some transformation relationships among these products. With the development of the reactions *in vivo*, drug metabolites were also enriched step by step. This "metabolite clusters" theory could better guide the screening of metabolites and reveal the metabolic process. However, these metabolites were also difficult to detect due to their low content, and many isomers were easily yielded in the biotransformation process (Wang et al., 2019). Therefore, it is urgent to establish high performance testing instruments and comprehensive and accurate analysis methods to help solve such problems.

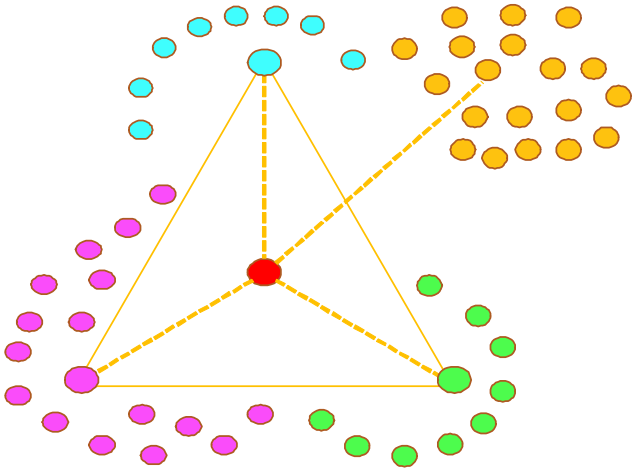

Fig. 6 The metabolite cluster model of resveratrol in rats. (Note: The color that these compounds represent are corresponding between Fig. 5 and Fig. 6).

4. Conclusion

In this study, three methods of biological sample preparation were applied to analyse the *in vivo* metabolism of resveratrol in rats. It's noted that SPE cartridge could remove matrix effect better. Meanwhile, the automation of SPE cartridge was helpful to process analysis of massive biological samples, which presented some advantages in saving time and working efficiently. Finally, a total of 56 resveratrol metabolites were detected and identified by the UHPLC-HRMS method. Among them, 39 metabolites were found in rat urine, 6 metabolites were detected in rat plasma, and 16 metabolites were characterized from rat faeces. The discrepancy in the number of metabolites detected might be due to the different metabolic transformation ability of phase II in plasma, urine and feces. At the same time, the intermediate and final metabolites formed a metabolite cluster, which was set in the triangular pyramid model, which revealed the potential pharmacodynamics forms of resveratrol.

In addition, the distinguishment of some isomers is still a challenge, which needs to pay more attention in the following researches. The ESI-MS/MS spectra fragmentation information with some other information such as the ClogP value to determine the possible position of substituents are much more logical technique. In a word, the present results not only supplied useful data for a better understanding of further research on resveratrol but also provided ideas and analysis for metabolites of other compounds.

Acknowledgments

This work has been financially supported by Young and Creative Team for Talent Introduction of Shandong Province, Binzhou Medical University Scientific Research Fund for High-level Talents (2019KYQD06), Locality-University Cooperation Project of Yantai City (2019XDRHXMPT18).

Declaration of Competing Interest

There are no conflicts of interest to declare.

References

Bergman, M., Levin, G.S., Bessler, H., et al, 2013. Resveratrol affects the cross talk between immune and colon cancer cells. Biomed. Pharmacother. 67, 43–47.

Boocock, D.J., Patel, K.R., Faust, G.E.S., et al, 2007. Quantitation of trans-resveratrol and detection of its metabolites in human plasma and urine by high performance liquid chromatography. J. Chromatogr. B 848, 182–187.

Chen, M., Fu, Q., Song, X., et al, 2020. Preparation of resveratrol dry suspension and its immunomodulatory and anti-inflammatory activity in mice. Pharm Bio. 58, 8–15.

Dai, S.Y., Shang, Z.P., Wang, F., et al, 2017. Novelty application of multi-omics correlation in the discrimination of sulfur-fumigation and non-sulfur-fumigation Ophiopogonis Radix. Sci. Rep.-UK 7, 9971.

Emília Juan, M., Maijó, M., Joana, M., 2010. Planas. Quantification of trans-resveratrol and its metabolites in rat plasma and tissues by HPLC. J. Pharm. Biomed. 70, 391–398.

Fremont, L., 2000. Biological effects of resveratrol. Life Sci. 6, 663–667.

Fu, L.L., Ding, H., Han, L.F., et al, 2019. Simultaneously targeted and untargeted multicomponent characterization of Erzhi Pill by offline two-dimensional liquid chromatography/quadrupole-Orbitrap mass spectrometry. J. Chromatogr. A 1584, 87–96.

Fu, J., Wu, S., Wang, M., et al, 2018. Intestinal Metabolism of Polygonum Cuspidatum in vitro and in vivo. Biomed. Chromatogr. 32, 4190.

Jordan, T.B., Nichols, D.S., Kerr, N.I., 2009. Selection of SPE cartridge for automated solid-phase extraction of pesticides from water followed by liquid chromatography-tandem mass spectrometry. Anal. Bioanal. Chem. 394, 2257–2266.

Mei, X.D., Wang, Y.Q., Li, J., et al, 2019. Comprehensive metabolism study of polydatin in rat plasma and urine using ultra-high performance liquid chromatography coupled with high-resolution mass spectrometry. J. Chromatogr. B 1117, 22–35.

Nema, T., Chan, E.C.Y., Ho, P.C., 2010. Application of silica-based monolith as solid phase extraction cartridge for extracting polar compounds from urine. Talanta 82.

Pan, H.Q., Zhou, H., Miao, S., et al, 2020. An integrated approach for global profiling of multi-type constituents: Comprehensive chemical characterization of Lonicerae Japonicae Flos as a case study. J. Chromatogr. A 1613, 460674.

Patel, K.R., Brown, V.A., Jones, D.J.L., et al, 2010. Clinical pharmacology of resveratrol and its metabolites in colorectal cancer patients. Cancer Res. 70, 7392–7399.

Samarjit, D., Dipak, K.D., 2007. Anti-inflammatory responses of resveratrol. Inflammation. 6, 168–173.

Sandermann, Heinrich, 1992. Plant metabolism of xenobiotics. Trends Biochem. Sci. 17, 82–84.

Shang, Z., Cai, W., Cao, Y., et al, 2017. An integrated strategy for rapid discovery and identification of the sequential piperine metabolites in rats using ultra high-performance liquid chromatography/high resolution mass spectrometery. J. Pharmaceut. Biomed. 146, 387.

Svajger, Urban, Jeras, M., 2012. Anti-inflammatory effects of resveratrol and its potential use in therapy of immune-mediated diseases. Int. Rev. Immunol. 31, 202–222.

Wang, D., Hang, T., Wu, C., et al, 2005. Identification of the major metabolites of resveratrol in rat urine by HPLC-MS/MS. J. Chromatogr. B 829, 97–106.

Wang, Y.Q., Mei, X.D., Liu, Z.H., et al, 2019. Drug metabolite cluster-Based data-mining method for comprehensive metabolism study of 5-hydroxy-6,7,3′,4′-tetramethoxyflavone in Rats. Molecules 2, 3278.

Wilkinson, G.R., 2005. Drug metabolism and variability among patients in drug response. N. Engl. J. Med. 352, 2211–2221.

Xu, B.P., Yao, M., Li, Z.J., et al, 2020. Neurological recovery and antioxidant effects of resveratrol in rats with spinal cord injury: a meta-analysis. Neural. Regen. Res. 3.

Xu, C., Li, Y.T., Kong, A.N.T., 2005. Induction of phase I, II and III drug metabolism/transport by xenobiotics. Arch. Pharm. Res. 28, 49–268.

Xu, L.L., Guo, F.X., Chi, S.S., et al, 2017. Rapid screening and identification of diterpenoids in tinospora sinensis based on high-performance liquid chromatography coupled with linear ion trap-orbitrap mass spectrometry. Molecules 22, 912.

Zhang, J.Y., Wang, Z.J., Zhang, Q., et al, 2014. Rapid screening and identification of target constituents using full scan-parent ions list-dynamic exclusion acquisition coupled to diagnostic product ions analysis on a hybrid LTQ-Orbitrap mass spectrometer. Talanta 124, 111–122.

Zhang, W., Li, Q., Zhu, M., et al, 2008. Direct determination of polydatin and its metabolite in rat excrement samples by high-performance liquid chromatography. Chem. Pharm. Bull. 56, 1592–1595.

Zhou, S., Yang, R., Teng, Z., et al, 2009. Dose-dependent absorption and metabolism of trans-polydatin in rats. J. Agric. Food Chem. 57, 4572–4579.